

# Dynamic Modeling and Analysis of a Self Voltage Regulating Three Phase Self-Excited Induction Generator

[<sup>1</sup>] M. Rizwan Khan, [<sup>2</sup>] M. Faisal Khan

[<sup>1</sup>] Department of Electrical Engineering, Aligarh Muslim University, Aligarh (U.P.)-202002 ,

[<sup>2</sup>] Electrical Engineering Section, University Polytechnic, Aligarh Muslim University, Aligarh (U.P.)-202002

**Abstract:-** Dynamic modeling and analysis of a self-voltage regulating, short shunt three-phase self-excited induction generator (SEIG) is undertaken in this paper. The derived d-q model of SEIG is implemented in terms of a simulation model to carry out its performance analysis under no-load and loading conditions. To assess the performance of a practically viable operation, the resistive-inductive (RL) load of 0.9 lagging power factor is considered for assessing SEIG performance. In order to establish the veracity of proposed analysis, the simulated results are experimentally verified.

**Index terms –** Six-phase SEIG; Self excited induction generator; RL load; Short shunt; SEIG test rig

## I. INTRODUCTION

Due to their squirrel cage construction, the self excited induction generators (SEIGs) offer rugged and fault tolerant operation which is the prime requirement in their field of application [1,2]. Foremost operating constraint associated with SEIGs is finding a tangible mean to fulfill their reactive power requirement [3]. Most conducive strategy in this regard has been to connect capacitances across their terminals to facilitate self excitation [4,5]. Equipped with optimum excitation capacitances, SEIG generates voltage across its terminals as soon as it is supplied required kinetic energy from the rotor side [6,7]. In turn, the rotor gets mechanical energy from a suitable prime mover such as a wind or mini/micro hydro turbine. SEIGs have inherently poor voltage regulation. Thus, in order to make them practically viable, SEIGs have to be able to self regulate their terminal load voltage. While various schemes may be considered in this regard [8]-[14], the one selected for the implementation should adhere to over all spirit of the SEIG system and must not adversely affect the ruggedness of the system. In this paper detailed d-q modeling, simulink implementation and performance analysis of a short shunt SEIG [4,12,15] is presented.

Nomenclature	
Symbol	Description
$R_s, R_r, R_L$	stator, rotor and load resistances ( $\Omega$ )
$L_{sl}, L_{rl}$	stator & rotor leakage inductances (H)
$\Psi_{sd}, \Psi_{sq}$	d and q axes stator flux (Wb)
$\Psi_{rd}, \Psi_{rq}$	d and q axes rotor flux (Wb)
$\Psi_{rd0}, \Psi_{rq0}$	d and q axes initial rotor flux (Wb)
$V_{dcap}, V_{acap}$	d and q axes instantaneous voltages across excitation capacitance (V).
$V_{dcsc}, V_{acsc}$	d and q axes instantaneous voltages across series capacitance (V).
$V_{qcap}^0, V_{dcap}^0$	constants representing d and q axes voltages due to initial charge on excitation capacitances (V)
$V_{rq}^0, V_{rd}^0$	constants representing rotor induced voltages along d and q axes due to remnant flux of rotor (V)
$V_L$	load voltage (V)
$L_m$	magnetizing inductance (H)
$L_L$	load inductance (H)
$I_L$	load Current (A)
$i_{dcap}, i_{acap}$	d and q axes capacitor currents (A)
$i_{sd}, i_{sq}$	d and q axes stator currents (A)
$i_{rd}, i_{rq}$	d and q axes rotor currents (A)
$i_{Ld}, i_{Lq}$	d and q axes load currents (A)
$I_s$	stator current (A)
$I_m$	magnetizing current (A)
$I_c$	excitation capacitor current (A)
$\omega_r$	rotor electrical speed (rads/sec)

**II. MODELING OF SEIG**

The d-q model of a three phase short shunt SEIG is depicted in Fig. 1[15,16]. The mathematical model of an induction machine in generation mode can be represented by (1) [15,16].

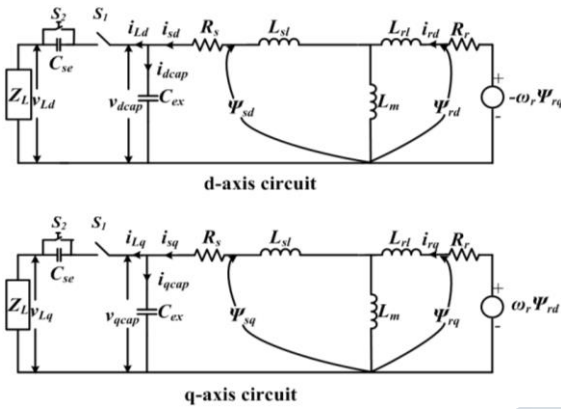


**Fig. 1 d-q model of a three phase SEIG**

$$p \begin{bmatrix} i_{sq} \\ i_{sd} \\ i_{rq} \\ i_{rd} \end{bmatrix} = -\frac{1}{L_m^2 L_r L_s} \begin{bmatrix} -L_r R_s & -L_m^2 \omega_r & L_m R_r & -L_m \omega_r L_r \\ L_m^2 \omega_r & -L_s R_s & L_m \omega_r L_r & L_m R_r \\ L_m R_s & L_m \omega_r L_s & -L_s R_r & -L_r \omega_r L_s \\ -L_m \omega_r L_s & L_m R_s & -L_r \omega_r L_s & -L_s R_r \end{bmatrix} \begin{bmatrix} i_{sq} \\ i_{sd} \\ i_{rq} \\ i_{rd} \end{bmatrix} + \begin{bmatrix} -L_r & 0 & L_m & 0 \\ 0 & -L_r & 0 & L_m \\ L_m & 0 & -L_s & 0 \\ 0 & L_m & 0 & -L_s \end{bmatrix} \begin{bmatrix} v_{qcap} \\ v_{dcap} \\ v_{rq}^0 \\ v_{rd}^0 \end{bmatrix} \quad (1)$$

In (2) to (4) some of the variables represent machine parameters and may be calculated from the standard tests available for the same [17]. However, besides the standard machine parameters the magnetizing inductance  $L_m$  (which is dynamic for generator operation) and the stator and rotor induced voltages have to be found for the solution.

**Modeling of Excitation Capacitance**

$$v_{qcap} = \frac{1}{C_{ex}} \int i_{qcap} dt + V_{qcap}^0 \quad (2)$$

$$v_{dcap} = \frac{1}{C_{ex}} \int i_{dcap} dt + V_{dcap}^0 \quad (3)$$

Here,  $i_{dcap}=i_{sd}$  and  $i_{qcap}=i_{sq}$

**Modeling of Series Capacitance**

$$v_{dcse} = \frac{1}{C_{se}} \int i_{Ld} dt \quad (4)$$

$$v_{qcse} = \frac{1}{C_{se}} \int i_{Lq} dt \quad (5)$$

**Modeling of Load**

$$p i_{Lq} = \frac{v_{qcap}}{L_L} - \frac{R_L}{L_L} i_{Lq} - \frac{1}{L_L C_{se}} \int i_{Lq} dt \quad (6)$$

$$p i_{Ld} = \frac{v_{dcap}}{L_L} - \frac{R_L}{L_L} i_{Ld} - \frac{1}{L_L C_{se}} \int i_{Ld} dt \quad (7)$$

Now,  $i_{dcap}=i_{sd}-i_{Ld}$  and  $i_{qcap}=i_{sq}-i_{Lq}$ , thus:

$$v_{qcap} = \frac{1}{C_{ex}} \int (i_{sq}-i_{Lq}) dt + V_{qcap}^0 \quad (8)$$

$$v_{dcap} = \frac{1}{C_{ex}} \int (i_{sd}-i_{Ld}) dt + V_{dcap}^0 \quad (9)$$

$$v_{Lq} = v_{qcap} - v_{qcse} \quad (10)$$

$$v_{Ld} = v_{dcap} - v_{dcse} \quad (11)$$

**III. RESULTS AND DISCUSSION**

The experimental set-up details and the equipment parameters are given in Appendix. In this section no-load and load performance of machine is assessed.

**A. Selection of Optimum Capacitances and Extraction of Magnetizing Characteristic**

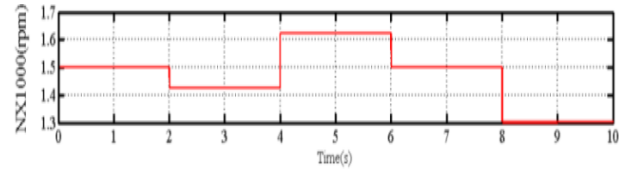
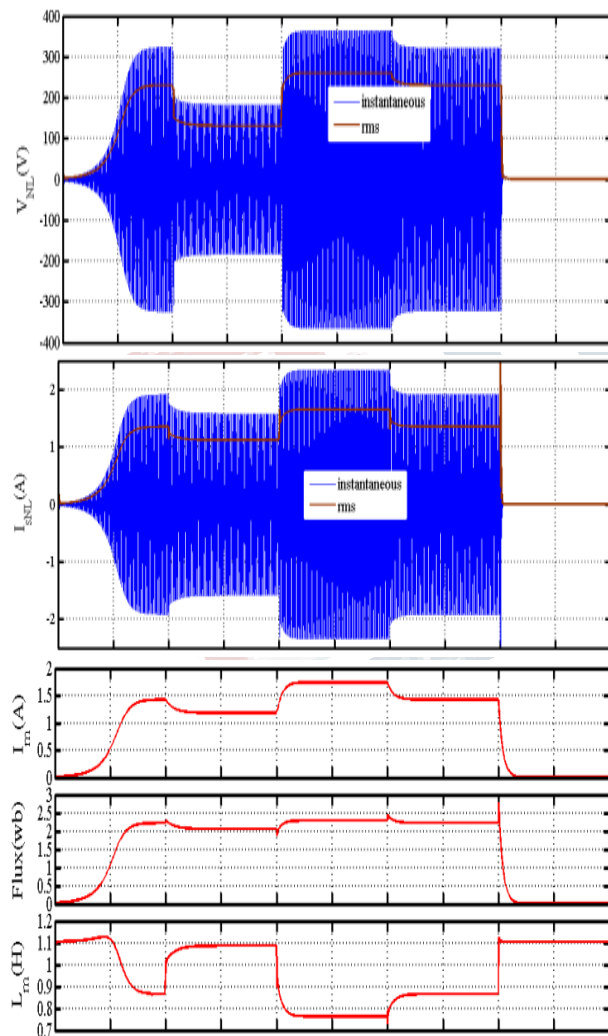
The optimum excitation (shunt) and the compensation (series) capacitances have been evaluated experimentally on the studied machine as 15  $\mu$ F (per phase) and 40  $\mu$ F respectively as they gave best voltage regulation at full load of unity pf. The magnetizing characteristic is evaluated through synchronous speed test [15]-[18] of the studied SEIG. The extracted magnetizing characteristic is given as:

$$L_m = -5.3635e^{-009} V_{ph}^3 - 1.8533e^{-007} V_{ph}^2 + 0.0029168 V_{ph} + 1.11034 \quad (12)$$

**B. Effect of Speed Variation on No-load Voltage**

The effect of speed variation on various SEIG parameters is assessed through the simulation results depicted in Fig. 3. For a marginal decrease in speed from 1500 rpm to

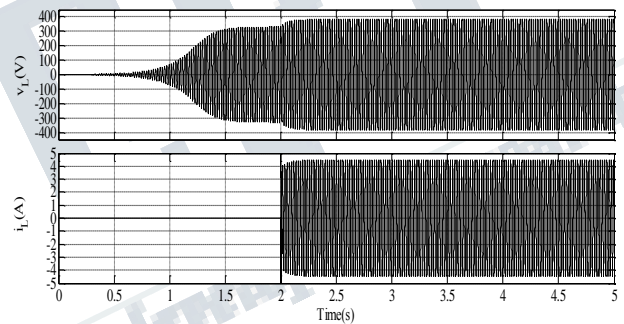
1422 rpm the generated no-load voltage drops to 135 V from the rated no load value of 230 V. This implies that for a drop in speed by about 5% of the rated value the generated no-load voltage drops by more than 58%. Also, it is seen that below 1420 rpm the SEIG loses excitation completely causing the voltage collapse. Alternately, when the speed is increased by 8% the generated voltage increases by 15 % to 265 V. Therefore, the change in generated voltage is sharper when the speed is decreased as against when it is increased. The variation in SEIG stator current attains the similar dynamics as the voltage.



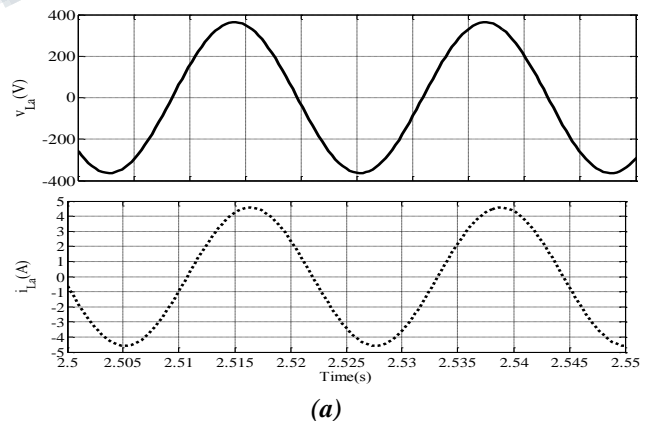
*Fig. 2. variation of SEIG parameters with speed.*

**C. SEIG Performance with 0.9 Lagging pf Loading**

Retaining the same set of optimum capacitances the rated load of 0.9 lagging power factor is switched to the SEIG terminals with  $R_L=76 \Omega$  and  $L_L=117 \text{ mH}$ . The simulated loading transients and the waveforms of load voltage and currents are depicted in Fig. 3 and Fig. 4 respectively. Here, it is seen that the SEIG operating in short shunt connection is able to supply the connected load successfully. The full load voltage is about 375 V (265 V, rms) and the load current attains a value of 4.67A (3.3 A, rms).



*Fig. 3. Loading transients for voltage and current at full load of 0.9 lagging pf.*



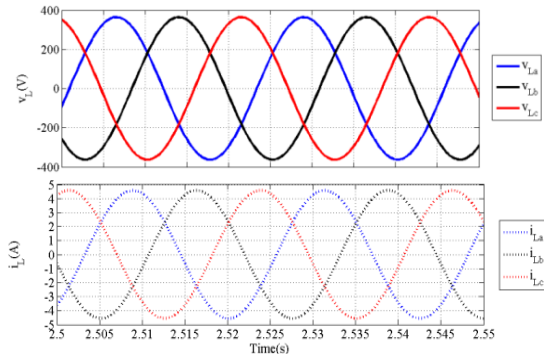


**Fig. 4. Zoomed view of load voltages at 0.9 lagging PF (a) phase a voltage and current (b) all three phase load voltages.**

The experimental results for the resistive-reactive (RL) loading considered for the simulation above are depicted in Fig. 5. It may be seen that load currents and voltages converge within  $\pm 5\%$  with the simulated results. Moreover, the three phase load voltages and currents are observed to be quite balanced as is evident from Fig. 5 (c). The measured active, reactive and the active powers may also be seen in Fig. 5(d).

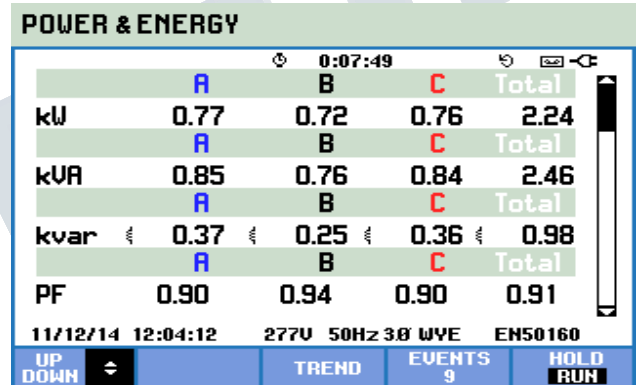
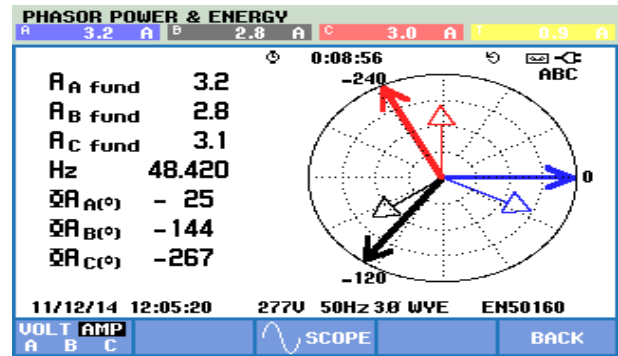
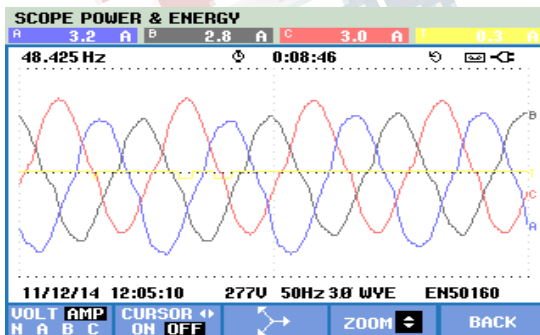
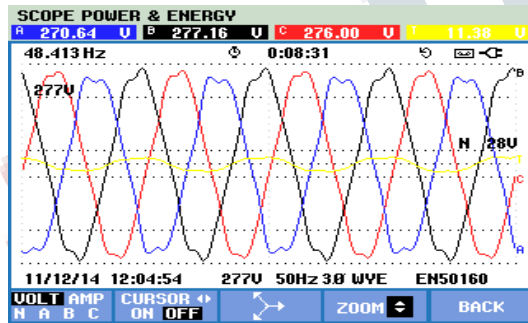


**Fig. 5. Measured output parameters of SEIG at rated load of 0.9 lagging power factor (a) three phase terminal load voltages (b) three phase load currents (c) phasors of load voltage and currents (d) active, reactive and apparent powers and operational power factor.**

#### IV. CONCLUSION

Mathematical modeling of a three-phase, self voltage regulating short shunt SEIG in stationary d-q reference frame is successfully demonstrated in this paper. The developed model is implemented in terms of a simulink model to carry out its no-load and on load analysis. The no-load results clearly show sensitivity of generated voltage to any transient change in driven speed. Subsequently, with the full load of 2.2 kW at 0.9 PF lagging being connected to the SEIG terminals, the SEIG is able to successfully withstand the loading and renders balanced output operation. The corresponding simulated and experimental results converge with 5% accuracy.



**REFERENCES**

- [1] L. A. C Lopes and R. G, Almeida, "Wind-driven self-excited induction generator with voltage and frequency regulated by a reduced-rating voltage source inverter," IEEE Trans. on Ene. Conv. , vol.21, no.2, pp.297,304, June 2006.
- [2] B. Thomsen, J. M. Guerrero, P. B. Thogersen, "Faroe islands wind-powered space heating microgrid using self-excited 220-kw induction generator", IEEE transactions on sustainable energy , vol.5, no.4, pp.1361-1366, Oct. 2014.
- [3] S. Kumar, N. M. Kumaresan, M. Subbiah, M. Rageeru, "Modelling, analysis and control of stand-alone self-excited induction generator-pulse width modulation rectifier systems feeding constant DC voltage applications", IET Generation, Transmission & Distribution, vol.8, no.6, pp.1140-1155, June 2014.
- [4] M.F. Khan, M.R. Khan, Analysis of voltage buildup and speed disturbance ride-through capability of a self excited induction generator for renewable energy application, International Journal of Power and Energy Conversion 7 (2016) 157-177.
- [5] Y. K. Chauhan, V. K. Yadav, B. Singh, "Optimum utilisation of self-excited induction generator", IET Electric Power Applications, vol.7, no.9, pp.680,692, November 2013.
- [6] M. F. Khan and M. R. Khan, "Wind Power Generation in India: Evolution, Trends and Prospects", International Journal of Renewable Energy Development, vol.2, no.3, pp. 175-186, 2013.
- [7] M. H. Haque, "A novel method of evaluating performance characteristics of a self-excited induction generator," IEEE Trans. Ene. Con., Vol. 24, No. 2, June 2009, pp. 358-365.
- [8] M. R. Khan, M. F. Khan and A. Iqbal "Investigation on Resonating Behaviour of a Self Excited Induction Generator", in the proceedings of IEEE Tencon-Spring 2013, 16-19 April'2013, Sydney, Australia.
- [9] R. R., Chilipi, B. Singh, S. S. Murthy, "Performance of a self-excited induction generator with dstatcom-dtc drive-based voltage and frequency controller", IEEE Transactions on Energy Conversion, vol.29, no.3, pp.545,557, Sept. 2014.
- [10] K. L. V. Iyer, Lu Xiaomin, Y. Usama, V. Ramakrishnan, N.C. Kar, "A twofold daubechies-wavelet-based module for fault detection and voltage regulation in seigs for distributed wind power generation", IEEE Transactions on Industrial Electronics, vol.60, no.4, pp.1638,1651, April 2013.
- [11] P. J. Chauhan , J.K. Chatterjee, H. Bhare , B.V. Perumal, D. Sarkar, "Synchronized operation of dsp-based generalized impedance controller with variable-speed isolated seig for novel voltage and frequency control", IEEE Transactions on Industry Applications, vol.51, no.2, pp.1845,1854, March-April 2015.
- [12] M. F. Khan and M. R. Khan, "Self regulating three phase-self excited induction generator for standalone generation," in Proc. IEEE INDICON 2013, pp.1-6, 13-15 Dec. 2013.
- [13] M. F. Khan and M. R. Khan, , "Voltage control of single-phase two winding self excited induction generator for isolated loads," Advances in Energy Conversion Technologies (ICAECT), 2014 International Conference on , vol., no., pp.209,214, 23-25 Jan. 2014  
IEEE Xplore doi: 10.1109/ICAECT.2014.6757089.
- [14] Y. K. Chauhan, S. K. Jain and B. Singh , "A prospective on voltage regulation of self-excited induction generators for industry applications," IEEE Trans. on Ind. Appl., vol.46, no.2, pp.720,730, March-april 2010.
- [15] M.F. Khan, Modeling and control of multi-phase induction generator for wind energy applications, Ph.D. Dissertation, Aligarh Muslim University, India (2015).
- [16] D. Seyoum, C. Grantham, M.F. Rahman, The dynamic characteristics of an isolated self-excited induction generator driven by a wind turbine, IEEE Transactions on Industry Applications 39 (2003) 936-944.

[17] G. B. Shrestha, M. H. Haque, "AC circuits and Machines", Singapore: Prentice-Hall, 2006.

[18] L. Kalamen, P. Rafajdus, P. Sekerák, and V. Harbovcová, "A novel method of magnetizing inductance investigation of self-excited induction generator," IEEE Trans. Mag., Vol. 48, No. 4, April 2012, pp. 1657-1660.

**APPENDIX**

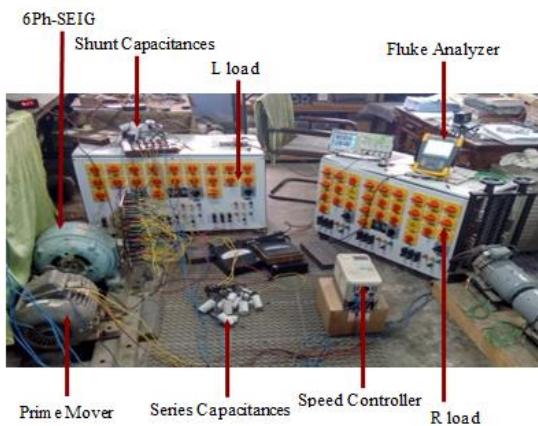


**Fig. 6. Illustration of the 6Ph-SEIG test-rig.**

**SEIG Parameters**

400 V, 3 hp/2.2KW, 5.5 A,  $R_s=5.3 \Omega$ ,  $R_r=1.7 \Omega$ ,  $X_{ls}=X_{lr}=5.45 \Omega$  open stator winding squirrel cage induction machine,

**Prime Mover Parameters**

3-phase, Delta connected, 415 V, 7.6 A, 3.7 KW, 1430 rpm, 50 Hz, Squirrel cage type induction motor.

**Speed Controller**

YASKAWA VARISPEED Inverter Drive 616G5, 3 phase, 400 V, 2.2 kW.